Supporting Information

Benzimidazole-based mononuclear polypyridyl Cu(II) complexes towards DNA binding, cleavage, and *in vitro* antiproliferative studies

Indrajit Roy[a], Shobhit Mathur[a], Sourav Deb[a], Sharan Shanmuga Vuppaladadium Rathnam[b], Nikhil Tuti[b], Unnikrishnan Paruthiyezhath Shaji[b], Karthikeyan L[a], Anindya Roy[b] and Somnath Maji[a]*

[a]Department of Chemistry, Indian Institute of Technology Hyderabad, Kandi, Sangareddy 502284, Telangana, India

[b]Department of Biotechnology, Indian Institute of Technology, Hyderabad, Kandi, Sangareddy 502284 Telangana, India

*Corresponding author

Email address: smaji@chy.iith.ac.in (Somnath Maji).

Table S1 Selected crystallographic data for **1**, **2** and **3**

Complex	**1**	**2**	**3**
Empirical formula	$C_{65}H_{61}Cl_4Cu_2N_{15}O_{19}$	$C_{35}H_{28}Cl_2CuN_8O_8$	$C_{35}H_{29}Cl_2CuN_7O_8$
Formula weight	1611.14	823.09	810.09
Temperature/K	298.00	298.00	298.00
Crystal system	triclinic	triclinic	monoclinic
Space group	*P*-1	*P*-1	$P2_1/c$
a/Å	8.9566(9)	9.1527(7)	13.4155(9)
b/Å	13.6649(12)	14.2703(11)	15.0657(10)
c/Å	29.392(3)	14.6239(11)	18.0834(10)
α/°	80.736(3)	90.791(3)	90
β/°	84.755(3)	99.831(3)	102.119(2)
γ/°	82.120(3)	108.495(2)	90
Volume/Å^3	3508.0(6)	1780.1(2)	3573.5(4)
Z	2	2	4
ρ_{calc}g/cm^3	1.525	1.536	1.506
μ/mm^{-1}	0.841	0.828	0.823
F(000)	1652.0	842.0	1660.0
Crystal size/mm^3	0.06 × 0.06 × 0.04	0.08 × 0.08 × 0.06	0.06 × 0.06 × 0.04
Radiation	MoKα (λ = 0.71073)	MoKα (λ = 0.71073)	MoKα (λ = 0.71073)
2*θ* range for data collection/°	3.54 to 54.206	3.986 to 54.206	3.552 to 54.43
Index ranges	−11 ≤ h ≤ 11, −16 ≤ k ≤ 17, −37 ≤ l ≤ 37	−11 ≤ h ≤ 11, −18 ≤ k ≤ 18, −18 ≤ l ≤ 18	−17 ≤ h ≤ 17, −19 ≤ k ≤ 19, −23 ≤ l ≤ 22
Reflections collected	110906	47026	57556
Independent reflections	15497 [R_{int} = 0.1390, R_{sigma} = 0.0947]	7817 [R_{int} = 0.0607, R_{sigma} = 0.0442]	7922 [R_{int} = 0.0883, R_{sigma} = 0.0588]
Data/restraints/parameters	15497/0/887	7817/0/462	7922/0/482
Goodness-of-fit on F^2	1.032	1.032	1.041
Final R indexes [I>=2σ (I)]	R_1 = 0.0643, wR_2 = 0.1565	R_1 = 0.0631, wR_2 = 0.1782	R_1 = 0.0733, wR_2 = 0.2067
Final R indexes [all data]	R_1 = 0.1304, wR_2 = 0.1845	R_1 = 0.0827, wR_2 = 0.1962	R_1 = 0.1260, wR_2 = 0.2440

Largest diff. peak/hole / e Å^{-3}	0.71/–0.50	1.57/–1.32	2.09/–0.73

Table S2 Selected bond lengths (Å) and bond angles (°) for **1**, **2** and **3**

Complex	**1**	**2**	**3**
Cu1–N1	1.964(3)	1.958(3)	1.964(4)
Cu1–N2	1.998(3)	2.006(3)	2.029(4)
Cu1–N3	2.014(3)	2.023(3)	2.020(4)
Cu1–N4	1.995(3)	1.991(3)	1.993(4)
Cu1–N5	2.192(3)	2.217(3)	2.202(4)
Cu2–N8	1.979(3)	-	-
Cu2–N9	2.031(3)	-	-
Cu2–N10	2.013(3)	-	-
Cu2–N11	2.210(4)	-	-
Cu2–N12	2.007(3)	-	-
N1–Cu1–N2	79.77(14)	80.07(12)	79.26(17)
N1–Cu1–N3	79.80(14)	79.57(12)	80.08(17)
N1–Cu1–N4	170.91(14)	174.03(11)	166.68(18)
N1–Cu1–N5	110.76(14)	106.82(12)	112.67(18)
N2–Cu1–N4	99.44(14)	99.06(12)	100.08(17)
N3–Cu1–N2	157.74(14)	157.68(12)	157.94(18)
N3–Cu1–N4	99.34(14)	100.24(12)	98.24(17)
N5–Cu1–N2	96.48(13)	99.67(12)	99.65(17)
N5–Cu1–N3	98.93(14)	94.88(12)	95.35(17)
N5–Cu1–N4	78.33(13)	79.15(11)	80.61(19)
N8–Cu2–N9	79.31(14)	-	-
N8–Cu2–N10	79.12(13)	-	-
N8–Cu2–N11	99.81(15)	-	-
N8–Cu2–N12	176.88(14)	-	-
N9–Cu2–N11	96.93(14)	-	-
N10–Cu2–N9	156.56(14)	-	-

N10–Cu2–N11	95.67(14)	-	-
N12–Cu2–N9	98.64(13)	-	-
N12–Cu2–N10	103.27(13)	-	-
N12–Cu2–N11	78.04(14)	-	-

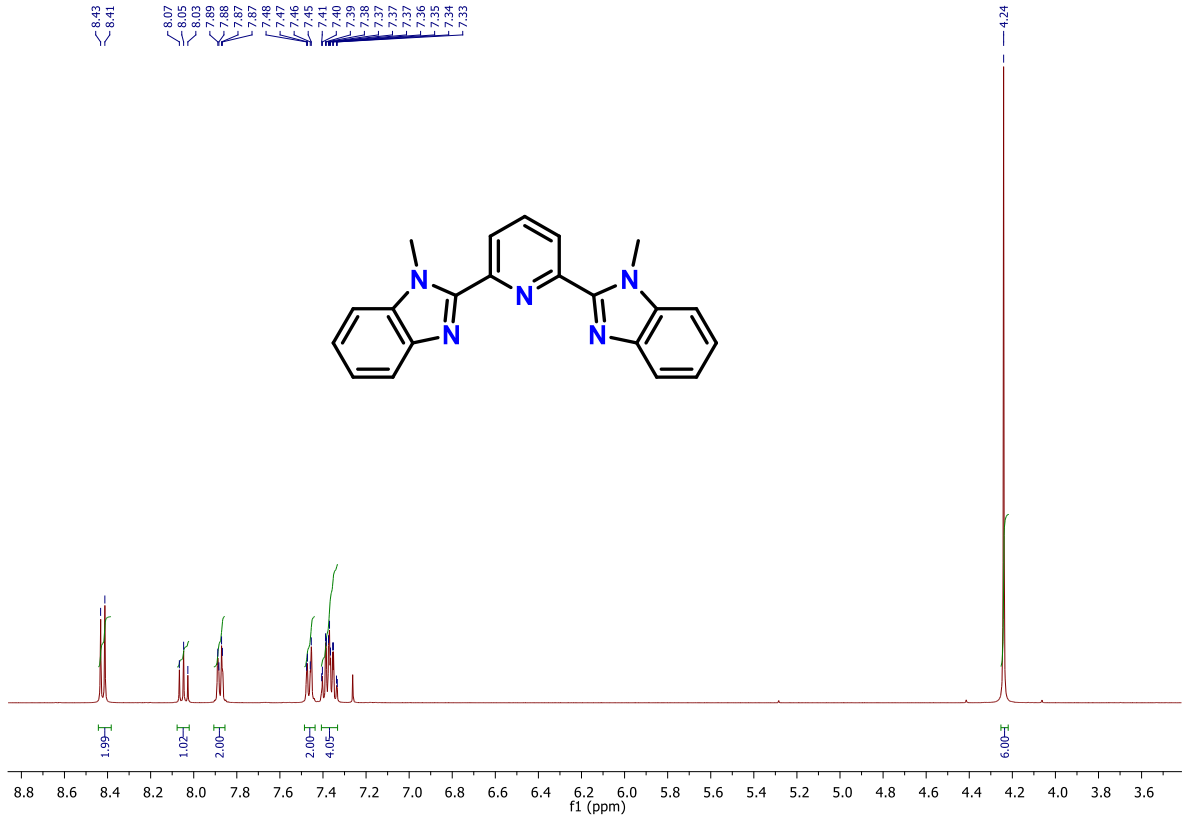

Fig. S1 ^{1}H NMR of ligand (**L**) in $CDCl_3$ at room temperature.

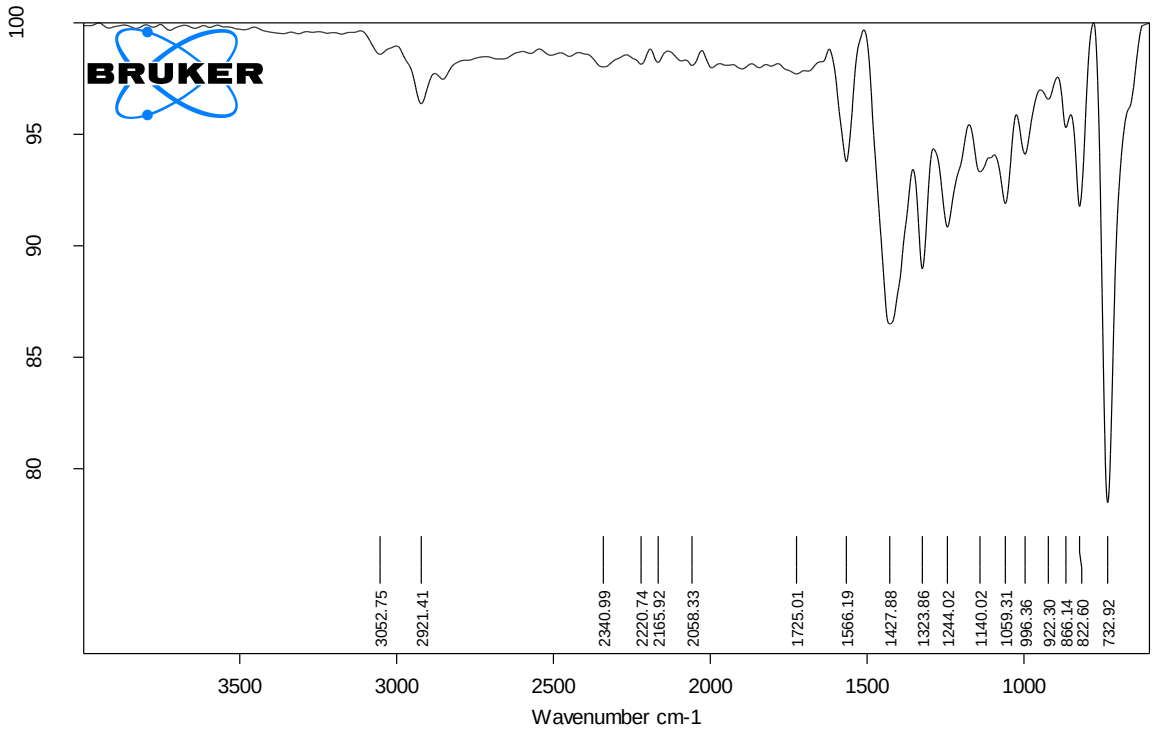

Fig. S2 FT-IR (solid) of **L**

a)

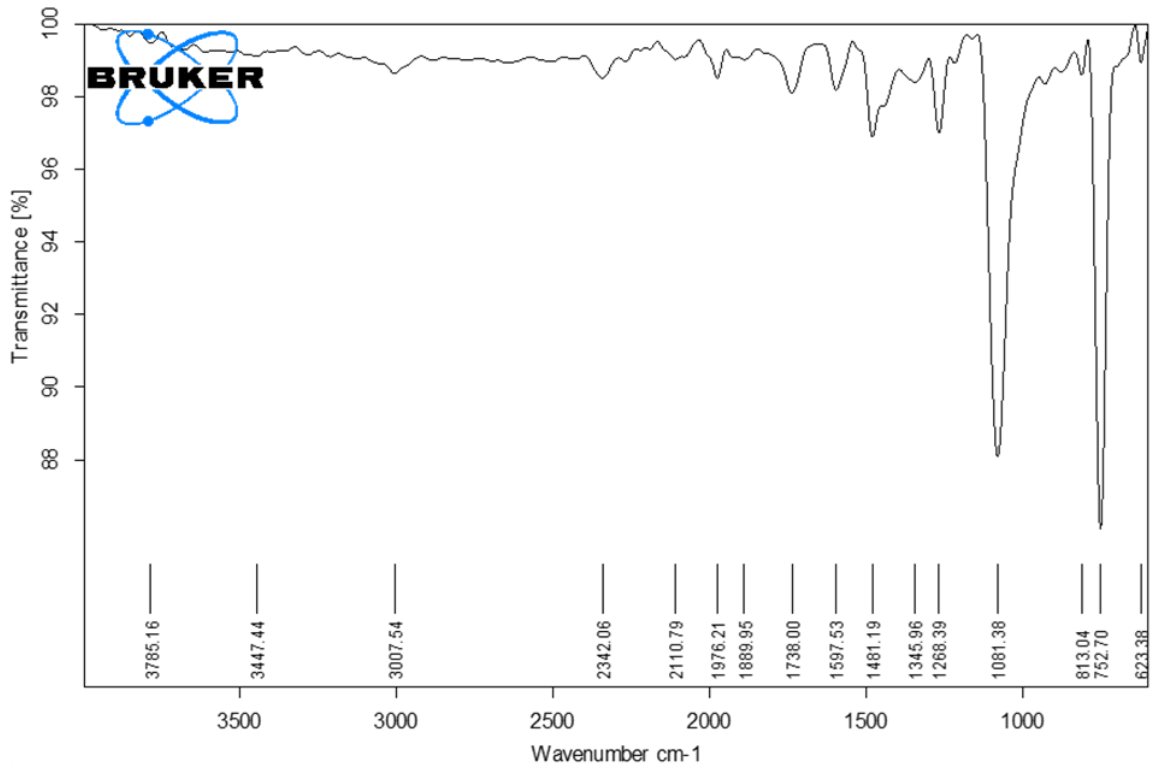

b)

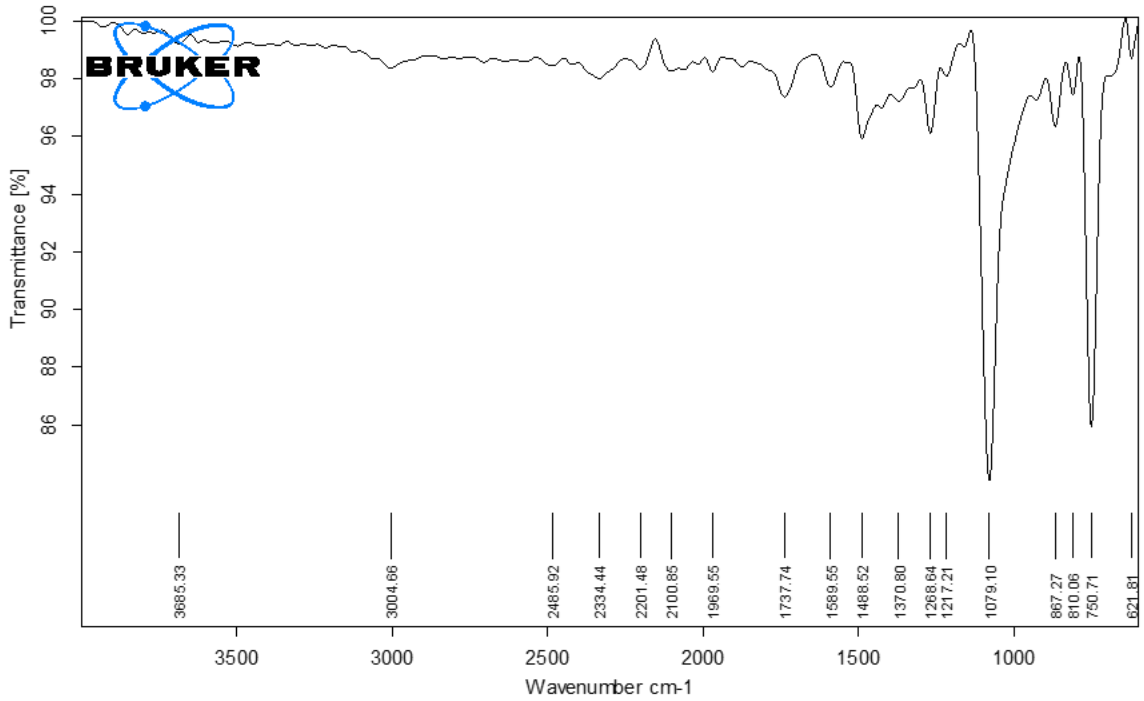

c)

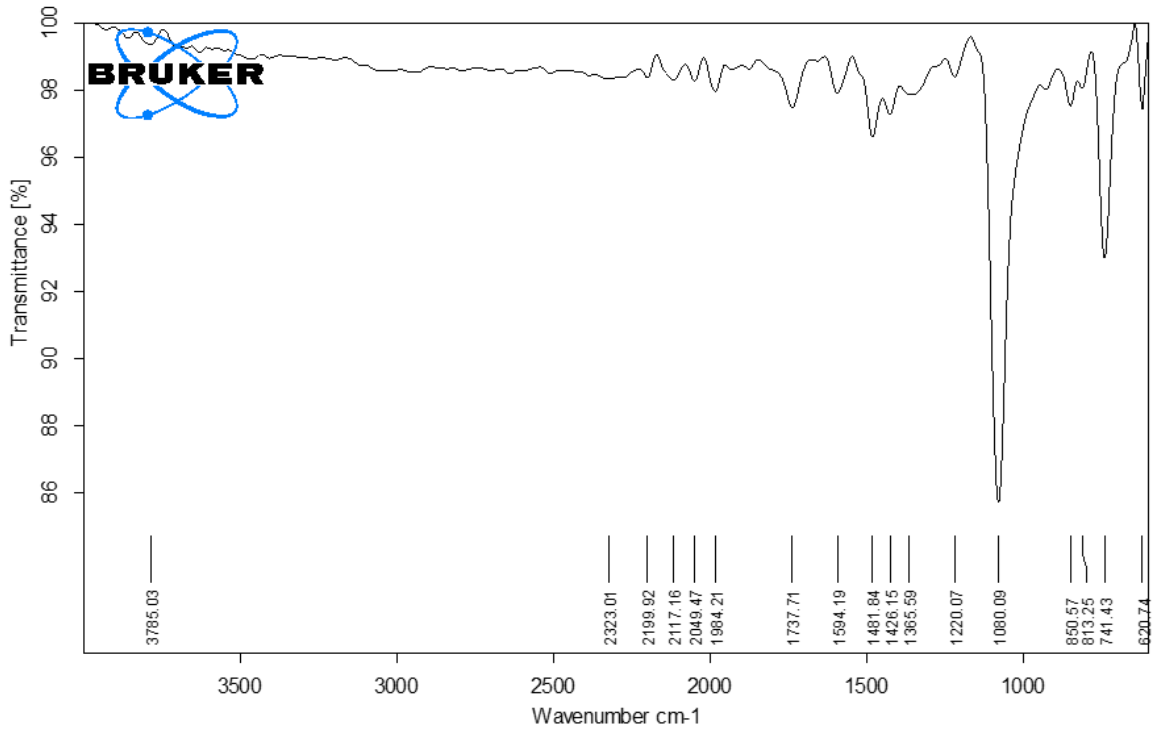

Fig. S3 FT-IR (solid) spectra of a) **1**, b) **2**, and c) **3**.

a)

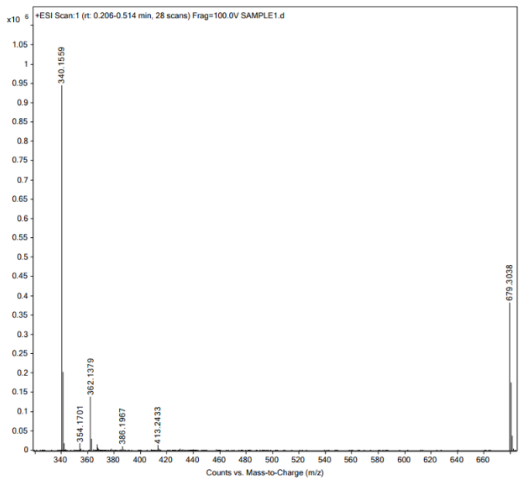
+ESI Scan:1 (rt: 0.206-0.514 min, 28 scans) Frag=100.0V SAMPLE1.d
340.1559
354.1701
362.1379
386.1967
413.2433
679.3038
Counts vs. Mass-to-Charge (m/z)

b)

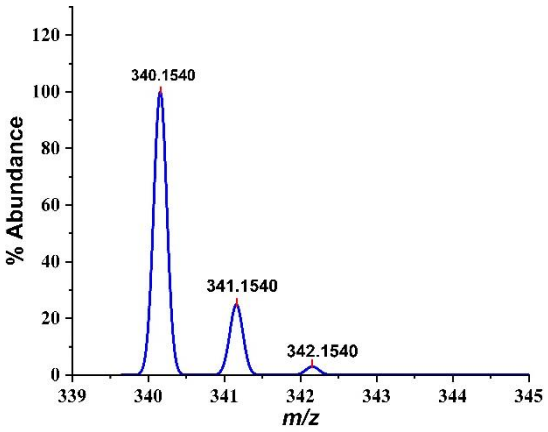
340.1540
341.1540
342.1540
% Abundance
m/z

c)

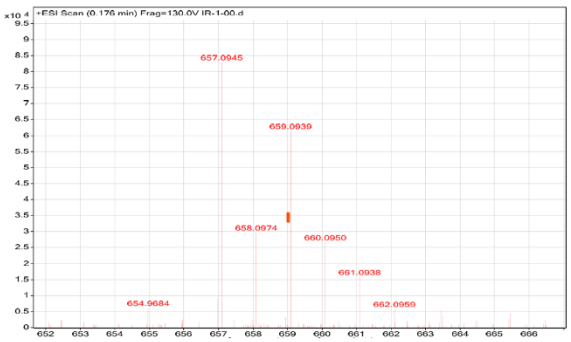
+ESI Scan (0.176 min) Frag=130.0V IR-1-00.d
657.0945
659.0939
658.0974
660.0950
661.0938
654.9684
662.0959

d)

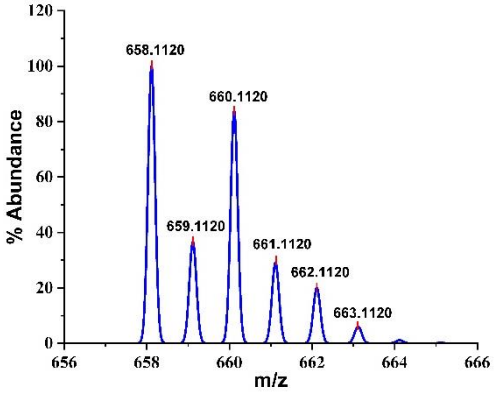
658.1120
660.1120
659.1120
661.1120
662.1120
663.1120
% Abundance
m/z

e)

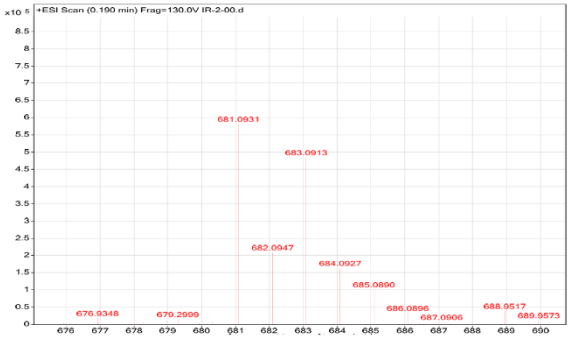
+ESI Scan (0.190 min) Frag=130.0V IR-2-00.d
681.0931
683.0913
682.0947
684.0927
685.0890
686.0896
687.0906
688.0517
689.0573
676.9348
679.2999

f)

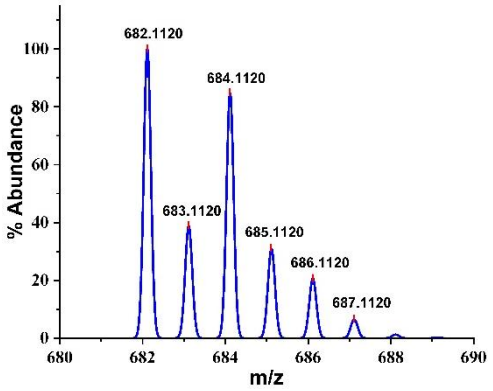
682.1120
684.1120
683.1120
685.1120
686.1120
687.1120
% Abundance
m/z

g) h)

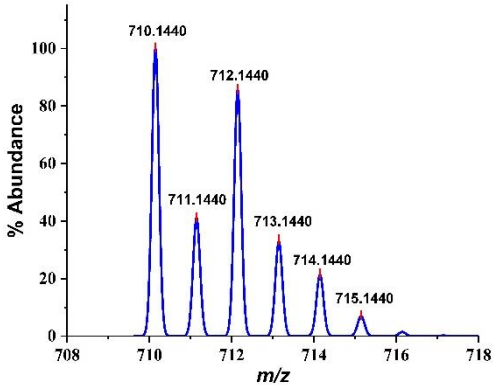

Fig. S4 HRMS spectra of the **L** a) experimental, b) simulated, **1** c) experimental, d) simulated, **2** e) experimental, f) simulated, and **3** g) experimental, h) simulated.

a)

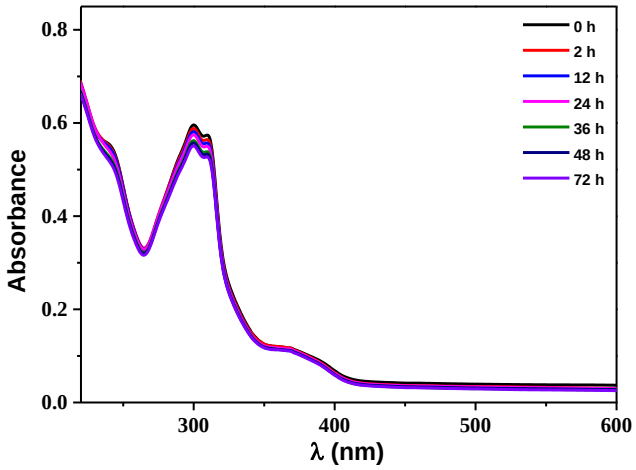

b)

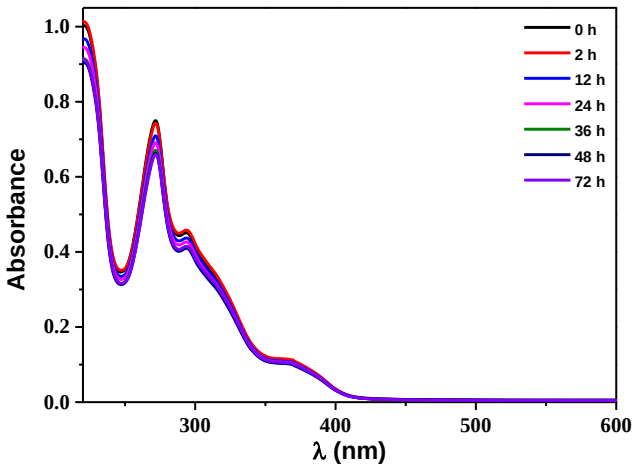

c)

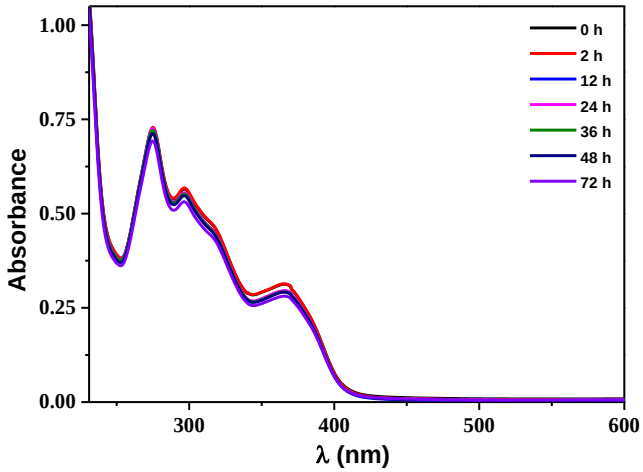

Fig. S5 Stability of (a) **1**, b) **2**, and (c) **3** in Tris-HCl buffer solution (pH 7.4) for three days.

a) b) c)

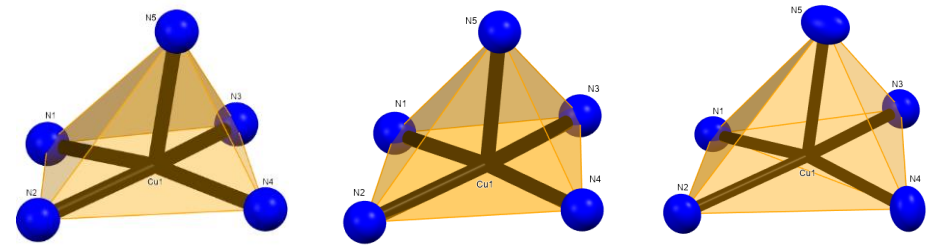

Fig. S6 Polyhedral view of a) **1**, b) **2** and c) **3**.

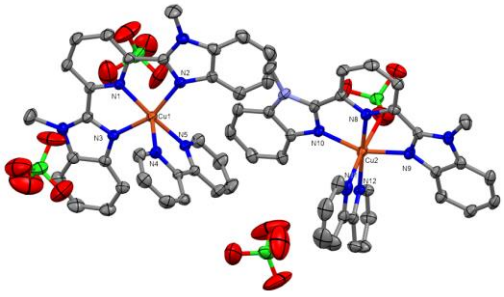

Fig. S7 The two non-equivalent Cu(II) units present in the crystal symmetry of **1**.

a)

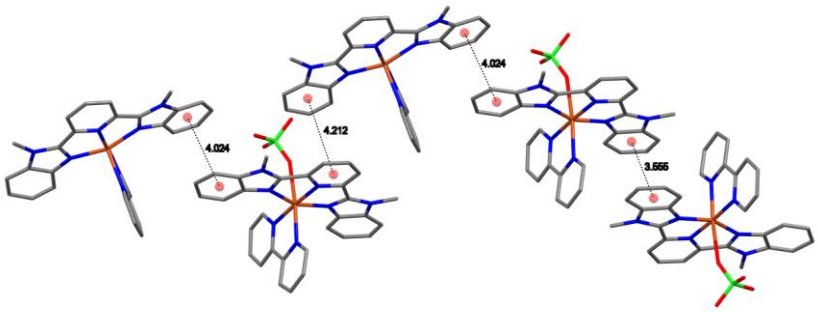

b)

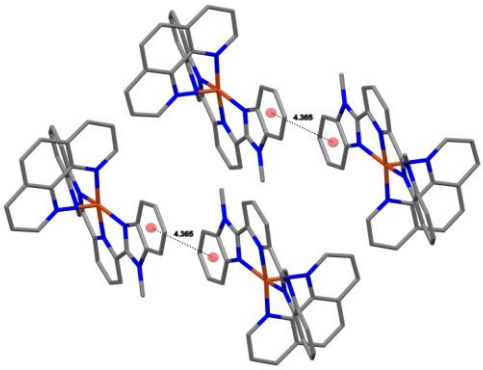

c)

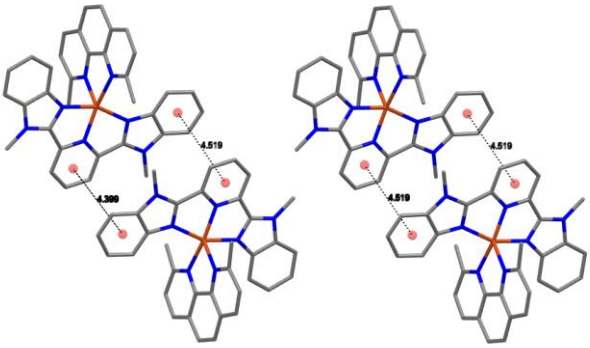

Fig. S8 Displaced π–π stacking interaction present in the crystal structures of a) **1**, b) **2** and c) **3**.

a)

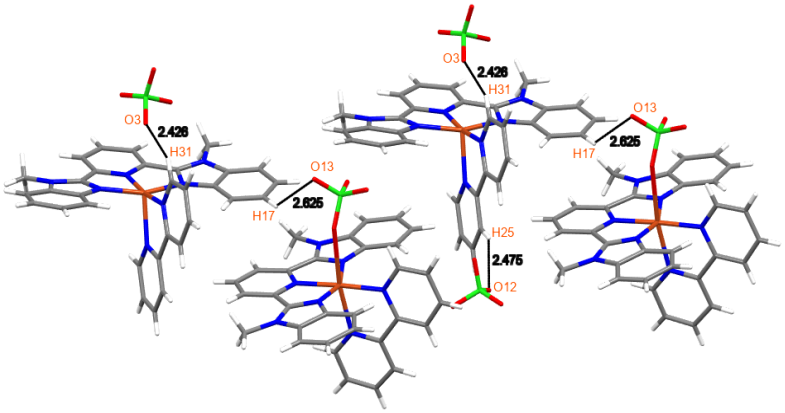

b)

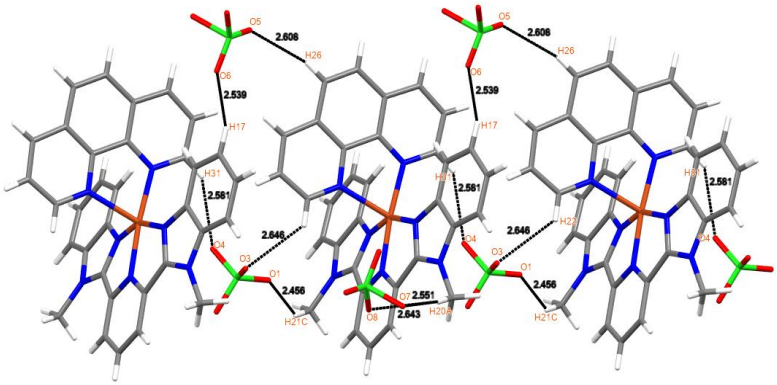

c)

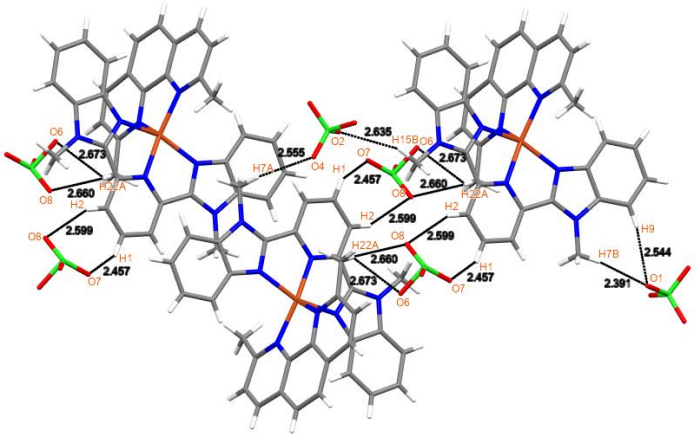

Fig. S9 Intermolecular H-bonding interactions present in the crystal symmetry of a) **1**, b) **2** and c) **3**.

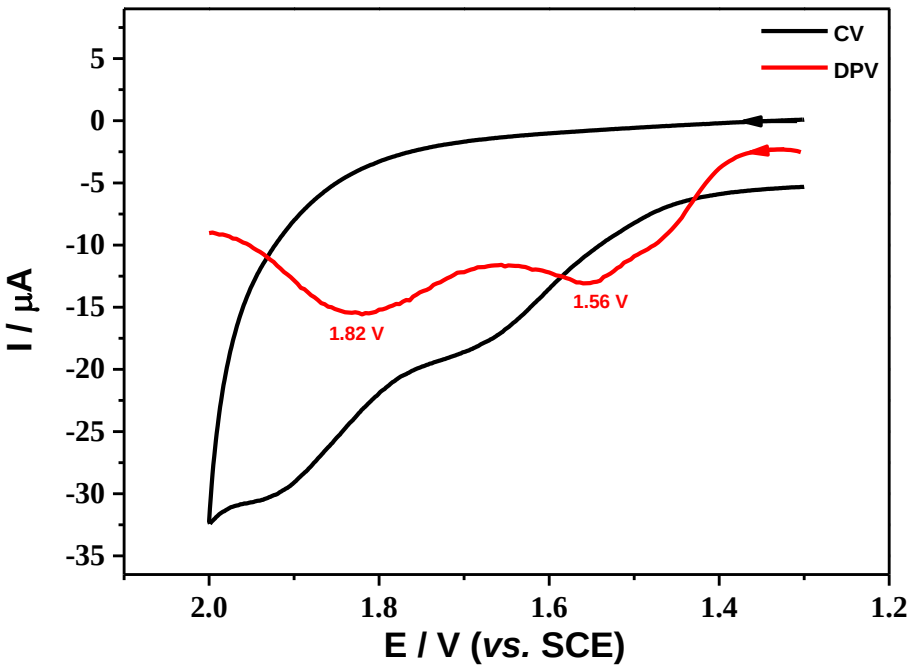

Fig. S10 CV (black line) and DPV (red line) of ligand **L** in dry acetonitrile solvent using 0.1 M TBAP as supporting electrolyte under nitrogen atmosphere at a scan rate of 100 mV s^{-1}.

a)

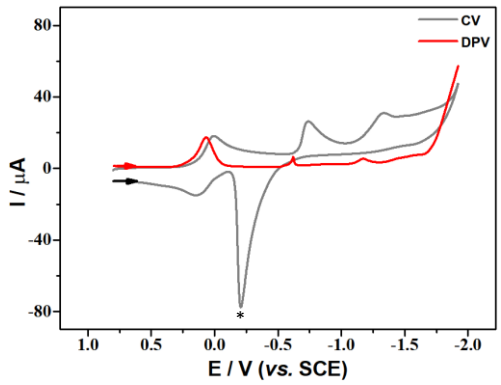

b)

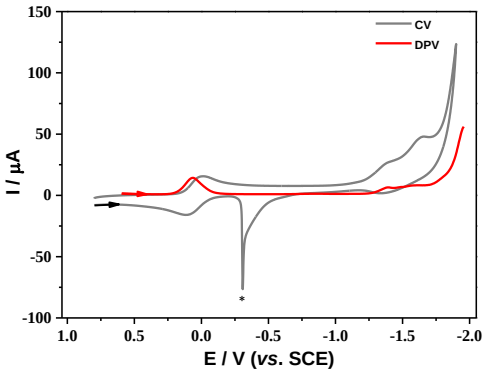

c)

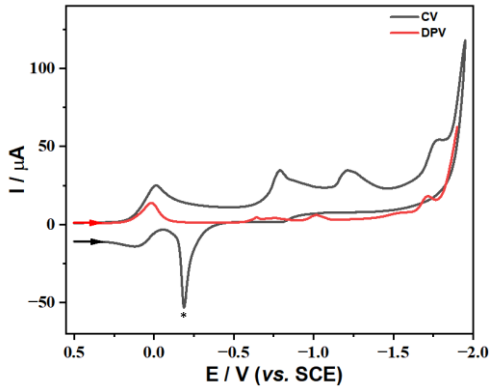

Fig. S11 CV (black line) and DPV (red line) of a) **1**, b) **2**, and b) **3** in dry acetonitrile solvent using 0.1 M TBAP as supporting electrolyte under nitrogen atmosphere. The * peak indicates the copper deposition on the electrode surface, for $Cu^0 \rightarrow Cu^I$ oxidation.